SINTEF
PROCEEDINGS
2

Proceedings of the 12th International Conference on Computational Fluid Dynamics in the Oil & Gas, Metallurgical and Process Industries

Progress in Applied CFD – CFD2017

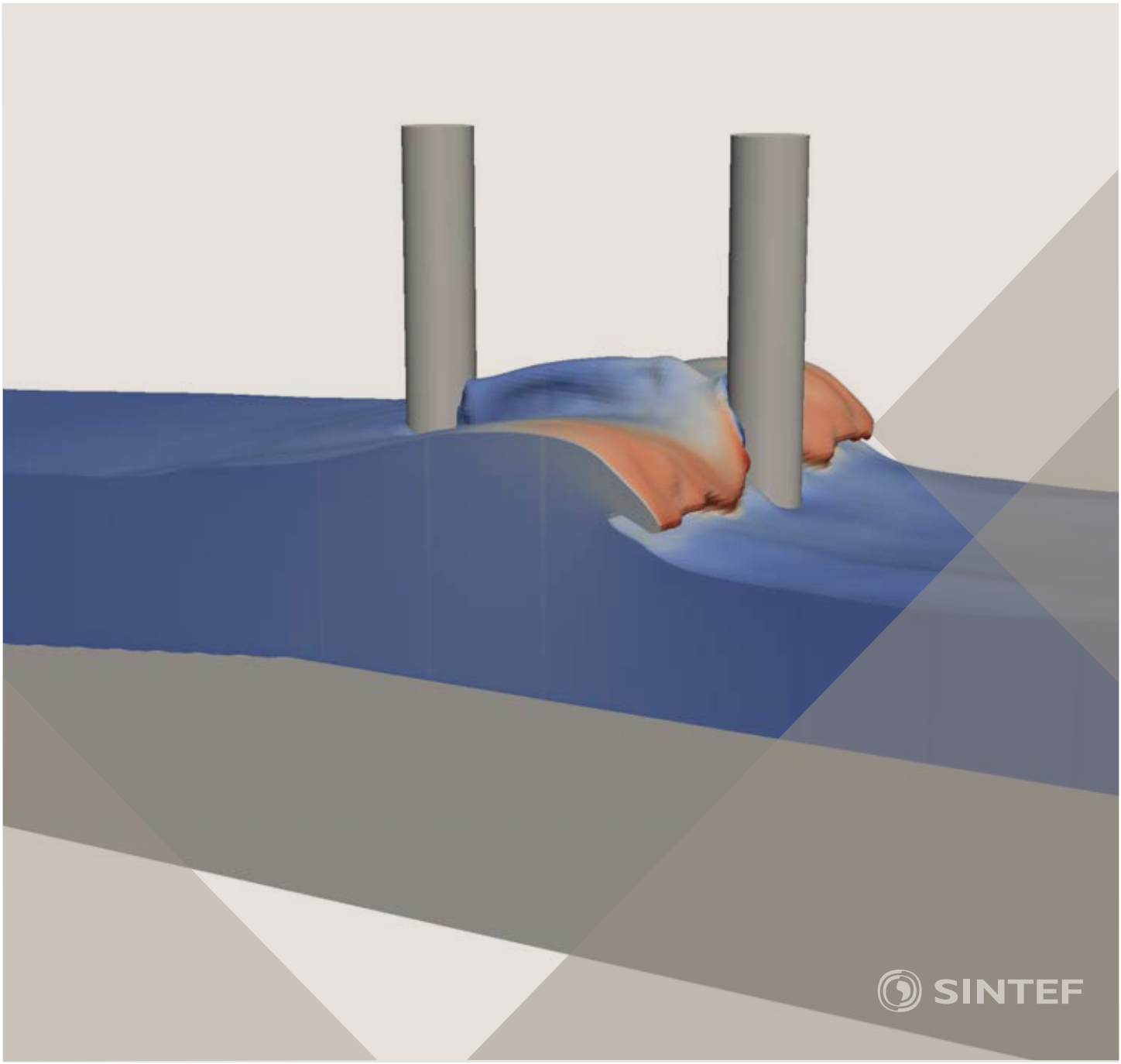

SINTEF Proceedings

Editors:
Jan Erik Olsen and Stein Tore Johansen

Progress in Applied CFD – CFD2017

Proceedings of the 12th International Conference on Computational Fluid Dynamics in the Oil & Gas, Metallurgical and Process Industries

SINTEF Academic Press

SINTEF Proceedings no 2
Editors: Jan Erik Olsen and Stein Tore Johansen
Progress in Applied CFD – CFD2017
Selected papers from 10th International Conference on Computational Fluid Dynamics in the Oil & Gas, Metallurgical and Process Industries

Key words:
CFD, Flow, Modelling

Cover, illustration: Arun Kamath

ISSN 2387-4295 (online)
ISBN 978-82-536-1544-8 (pdf)

SINTEF Academic Press
Address: Forskningsveien 3 B
PO Box 124 Blindern
N-0314 OSLO
Tel: +47 73 59 30 00
Fax: +47 22 96 55 08

www.sintef.no/byggforsk
www.sintefbok.no

SINTEF Proceedings
SINTEF Proceedings is a serial publication for peer-reviewed conference proceedings on a variety of scientific topics.
The processes of peer-reviewing of papers published in SINTEF Proceedings are administered by the conference organizers and proceedings editors. Detailed procedures will vary according to custom and practice in each scientific community.

PREFACE

This book contains all manuscripts approved by the reviewers and the organizing committee of the 12th International Conference on Computational Fluid Dynamics in the Oil & Gas, Metallurgical and Process Industries. The conference was hosted by SINTEF in Trondheim in May/June 2017 and is also known as CFD2017 for short. The conference series was initiated by CSIRO and Phil Schwarz in 1997. So far the conference has been alternating between CSIRO in Melbourne and SINTEF in Trondheim. The conferences focuses on the application of CFD in the oil and gas industries, metal production, mineral processing, power generation, chemicals and other process industries. In addition pragmatic modelling concepts and bio-mechanical applications have become an important part of the conference. The papers in this book demonstrate the current progress in applied CFD.

The conference papers undergo a review process involving two experts. Only papers accepted by the reviewers are included in the proceedings. 108 contributions were presented at the conference together with six keynote presentations. A majority of these contributions are presented by their manuscript in this collection (a few were granted to present without an accompanying manuscript).

The organizing committee would like to thank everyone who has helped with review of manuscripts, all those who helped to promote the conference and all authors who have submitted scientific contributions. We are also grateful for the support from the conference sponsors: ANSYS, SFI Metal Production and NanoSim.

Stein Tore Johansen & Jan Erik Olsen

Organizing committee:

Conference chairman: Prof. Stein Tore Johansen
Conference coordinator: Dr. Jan Erik Olsen
Dr. Bernhard Müller
Dr.Sigrid Karstad Dahl
Dr.Shahriar Amini
Dr.Ernst Meese
Dr.Josip Zoric
Dr.Jannike Solsvik
Dr.Peter Witt

Scientific committee:

Stein Tore Johansen, SINTEF/NTNU
Bernhard Müller, NTNU
Phil Schwarz, CSIRO
Akio Tomiyama, Kobe University
Hans Kuipers, Eindhoven University of Technology
Jinghai Li, Chinese Academy of Science
Markus Braun, Ansys
Simon Lo, CD-adapco
Patrick Segers, Universiteit Gent
Jiyuan Tu, RMIT
Jos Derksen, University of Aberdeen
Dmitry Eskin, Schlumberger-Doll Research
Pär Jönsson, KTH
Stefan Pirker, Johannes Kepler University
Josip Zoric, SINTEF

CONTENTS

PRAGMATIC MODELLING 9
On pragmatism in industrial modeling. Part III: Application to operational drilling 11
CFD modeling of dynamic emulsion stability 23
Modelling of interaction between turbines and terrain wakes using pragmatic approach 29

FLUIDIZED BED 37
Simulation of chemical looping combustion process in a double looping fluidized bed reactor with cu-based oxygen carriers 39
Extremely fast simulations of heat transfer in fluidized beds 47
Mass transfer phenomena in fluidized beds with horizontally immersed membranes 53
A Two-Fluid model study of hydrogen production via water gas shift in fluidized bed membrane reactors 63
Effect of lift force on dense gas-fluidized beds of non-spherical particles 71
Experimental and numerical investigation of a bubbling dense gas-solid fluidized bed 81
Direct numerical simulation of the effective drag in gas-liquid-solid systems 89
A Lagrangian-Eulerian hybrid model for the simulation of direct reduction of iron ore in fluidized beds 97
High temperature fluidization - influence of inter-particle forces on fluidization behavior 107
Verification of filtered two fluid models for reactive gas-solid flows 115

BIOMECHANICS 123
A computational framework involving CFD and data mining tools for analyzing disease in cartoid artery 125
Investigating the numerical parameter space for a stenosed patient-specific internal carotid artery model 133
Velocity profiles in a 2D model of the left ventricular outflow tract, pathological case study using PIV and CFD modeling 139
Oscillatory flow and mass transport in a coronary artery 147
Patient specific numerical simulation of flow in the human upper airways for assessing the effect of nasal surgery 153
CFD simulations of turbulent flow in the human upper airways 163

OIL & GAS APPLICATIONS 169
Estimation of flow rates and parameters in two-phase stratified and slug flow by an ensemble Kalman filter 171
Direct numerical simulation of proppant transport in a narrow channel for hydraulic fracturing application 179
Multiphase direct numerical simulations (DNS) of oil-water flows through homogeneous porous rocks 185
CFD erosion modelling of blind tees 191
Shape factors inclusion in a one-dimensional, transient two-fluid model for stratified and slug flow simulations in pipes 201
Gas-liquid two-phase flow behavior in terrain-inclined pipelines for wet natural gas transportation 207

NUMERICS, METHODS & CODE DEVELOPMENT 213
Innovative computing for industrially-relevant multiphase flows 215
Development of GPU parallel multiphase flow solver for turbulent slurry flows in cyclone 223
Immersed boundary method for the compressible Navier–Stokes equations using high order summation-by-parts difference operators 233
Direct numerical simulation of coupled heat and mass transfer in fluid-solid systems 243
A simulation concept for generic simulation of multi-material flow, using staggered Cartesian grids 253
A cartesian cut-cell method, based on formal volume averaging of mass, momentum equations 265
SOFT: a framework for semantic interoperability of scientific software 273

POPULATION BALANCE 279
Combined multifluid-population balance method for polydisperse multiphase flows 281
A multifluid-PBE model for a slurry bubble column with bubble size dependent velocity, weight fractions and temperature 285
CFD simulation of the droplet size distribution of liquid-liquid emulsions in stirred tank reactors 295
Towards a CFD model for boiling flows: validation of QMOM predictions with TOPFLOW experiments 301
Numerical simulations of turbulent liquid-liquid dispersions with quadrature-based moment methods 309
Simulation of dispersion of immiscible fluids in a turbulent couette flow 317
Simulation of gas-liquid flows in separators - a Lagrangian approach 325
CFD modelling to predict mass transfer in pulsed sieve plate extraction columns 335

BREAKUP & COALESCENCE 343
Experimental and numerical study on single droplet breakage in turbulent flow 345
Improved collision modelling for liquid metal droplets in a copper slag cleaning process 355
Modelling of bubble dynamics in slag during its hot stage engineering 365
Controlled coalescence with local front reconstruction method 373

BUBBLY FLOWS 381
Modelling of fluid dynamics, mass transfer and chemical reaction in bubbly flows 383
Stochastic DSMC model for large scale dense bubbly flows 391
On the surfacing mechanism of bubble plumes from subsea gas release 399
Bubble generated turbulence in two fluid simulation of bubbly flow 405

HEAT TRANSFER 413
CFD-simulation of boiling in a heated pipe including flow pattern transitions using a multi-field concept 415
The pear-shaped fate of an ice melting front 423
Flow dynamics studies for flexible operation of continuous casters (flow flex cc) 431
An Euler-Euler model for gas-liquid flows in a coil wound heat exchanger 441

NON-NEWTONIAN FLOWS 449
Viscoelastic flow simulations in disordered porous media 451
Tire rubber extrudate swell simulation and verification with experiments 459
Front-tracking simulations of bubbles rising in non-Newtonian fluids 469
A 2D sediment bed morphodynamics model for turbulent, non-Newtonian, particle-loaded flows 479

METALLURGICAL APPLICATIONS 491
Experimental modelling of metallurgical processes 493
State of the art: macroscopic modelling approaches for the description of multiphysics phenomena within the electroslag remelting process 499
LES-VOF simulation of turbulent interfacial flow in the continuous casting mold 507
CFD-DEM modelling of blast furnace tapping 515
Multiphase flow modelling of furnace tapholes 521
Numerical predictions of the shape and size of the raceway zone in a blast furnace 531
Modelling and measurements in the aluminium industry - Where are the obstacles? 541
Modelling of chemical reactions in metallurgical processes 549
Using CFD analysis to optimise top submerged lance furnace geometries 555
Numerical analysis of the temperature distribution in a martensic stainless steel strip during hardening 565
Validation of a rapid slag viscosity measurement by CFD 575
Solidification modeling with user defined function in ANSYS Fluent 583
Cleaning of polycyclic aromatic hydrocarbons (PAH) obtained from ferroalloys plant 587
Granular flow described by fictitious fluids: a suitable methodology for process simulations 593
A multiscale numerical approach of the dripping slag in the coke bed zone of a pilot scale Si-Mn furnace 599

INDUSTRIAL APPLICATIONS 605
Use of CFD as a design tool for a phospheric acid plant cooling pond 607
Numerical evaluation of co-firing solid recovered fuel with petroleum coke in a cement rotary kiln: Influence of fuel moisture 613
Experimental and CFD investigation of fractal distributor on a novel plate and frame ion-exchanger 621

COMBUSTION 631
CFD modeling of a commercial-size circle-draft biomass gasifier 633
Numerical study of coal particle gasification up to Reynolds numbers of 1000 641
Modelling combustion of pulverized coal and alternative carbon materials in the blast furnace raceway 647
Combustion chamber scaling for energy recovery from furnace process gas: waste to value 657

PACKED BED 665
Comparison of particle-resolved direct numerical simulation and 1D modelling of catalytic reactions in a packed bed 667
Numerical investigation of particle types influence on packed bed adsorber behaviour 675
CFD based study of dense medium drum separation processes 683
A multi-domain 1D particle-reactor model for packed bed reactor applications 689

SPECIES TRANSPORT & INTERFACES 699
Modelling and numerical simulation of surface active species transport - reaction in welding processes 701
Multiscale approach to fully resolved boundary layers using adaptive grids 709
Implementation, demonstration and validation of a user-defined wall function for direct precipitation fouling in Ansys Fluent 717

FREE SURFACE FLOW & WAVES 727
Unresolved CFD-DEM in environmental engineering: submarine slope stability and other applications 729
Influence of the upstream cylinder and wave breaking point on the breaking wave forces on the downstream cylinder 735
Recent developments for the computation of the necessary submergence of pump intakes with free surfaces 743
Parallel multiphase flow software for solving the Navier-Stokes equations 752

PARTICLE METHODS 759
A numerical approach to model aggregate restructuring in shear flow using DEM in Lattice-Boltzmann simulations 761
Adaptive coarse-graining for large-scale DEM simulations 773
Novel efficient hybrid-DEM collision integration scheme 779
Implementing the kinetic theory of granular flows into the Lagrangian dense discrete phase model 785
Importance of the different fluid forces on particle dispersion in fluid phase resonance mixers 791
Large scale modelling of bubble formation and growth in a supersaturated liquid 798

FUNDAMENTAL FLUID DYNAMICS 807
Flow past a yawed cylinder of finite length using a fictitious domain method 809
A numerical evaluation of the effect of the electro-magnetic force on bubble flow in aluminium smelting process 819
A DNS study of droplet spreading and penetration on a porous medium 825
From linear to nonlinear: Transient growth in confined magnetohydrodynamic flows 831

CLEANING OF POLYCYCLIC AROMATIC HYDROCARBONS (PAH) OBTAINED FROM FERROALLOYS PLANT

Balram Panjwani, Stefan Andersson, Bernd Wittgens, and Jan Erik Olsen

SINTEF Materials and Chemistry, 7465 Trondheim, NORWAY

* E-mail: balram.panjwani@sintef.no

ABSTRACT

Polycyclic Aromatic hydrocarbons (PAHs) are organic compounds consisting of only hydrogen and aromatic carbon rings. PAHs are neutral, non-polar molecules that are produced due to incomplete combustion of organic matter. These compounds are carcinogenic and interact with biological nucleophiles to inhibit the normal metabolic functions of the cells. In Norway, the most important sources of PAH pollution are considered to be metallurgical industries, offshore oil industries, transport and wood burning. Stricter governmental regulations regarding emissions to the outer and internal environment combined with increased awareness of the potential health effects have motivated Norwegian metal industries to increase their efforts to reduce emissions considerably. One of the objective of the ongoing industry and Norwegian research council supported "SCORE" project at SINTEF is to remove PAH from a hot gas stream through controlled combustion of the PAH inside a dedicated combustion chamber. The sizing and configuration of the combustion chamber depends on the properties of the bulk gas stream and the properties of the PAH itself. In order to achieve efficient and complete combustion of the PAH, the residence time and temperature need to be optimized. In the present study, the oxidation of pure PAH and PAH mixed with process gas is modelled using a Perfectly Stirred Reactor (PSR) concept. PSR concept was useful for understanding the influence of residence time and temperature on the oxidation of PAH to CO2 and water. Furthermore, a computationally fast approach based on Chemical Reactor Network (CRN) is proposed for understanding the oxidation of PAH inside complex geometries. The Chemical Reactor Network (CRN) yields a detailed composition regarding species and temperature in the combustion chamber.

Keywords: PAH, PSR, Energy recovery, Ferro alloy furnace

INTRODUCTION

Polycyclic Aromatic Hydrocarbons (PAHs) are one of the most stable classes of compounds and the largest organic chemical species known so far. It was in existence even before life started on Earth and it is considered to be one of the building blocks responsible for life on Earth. In the universe, PAH molecules are formed from carbon-rich, dying, giant red stars. These molecules grow in size and finally become larger dust particles. Formation of a nucleus takes place at around 2000 K and then the growth from nucleus to the larger PAH structure happen continuously. In Earth's atmosphere, PAHs are formed as a result of incomplete combustion of organic material or natural gas and also due to smoking and sometimes also natural processes such as carbonization. There are several hundred available PAHs and among them benzo[a]pyrene (BaP) is widely known and most frequently detected. The PAHs are found in air, water, food, and soil. In submerged arc furnaces, PAHs are major components formed during coal pyrolysis and combustion processes. Efficient pyrolysis of coal should result in the breakdown of large organic molecules to smaller hydrocarbons and in efficient combustion the only products should be CO_2, H_2O, CO etc. However, such complete degradation of coal rarely occurs and fairly large organic compounds, including PAHs, can be released from combustion sources. The formation of PAHs during coal combustion follows a complex pathway. Their formation depends on many variables such as temperature, oxygen concentration, and carbon-to-hydrogen ratio of the fuel. In principle it is difficult to control the PAH formation especially when the metal reduction processes take place inside the submerged arc furnace. Since controlling the formation of PAH is a challenge, a post-treatment of the PAH is therefore a viable option. There are many treatment methods for removal of PAH from liquids (e.g., liquid-liquid extraction, column liquid chromatography, and solid-phase extraction). However, few of these methods can be applied for efficient removal from gaseous streams (i.e., absorbent or adsorbent injection). Most of the available technologies are also expensive and some of them require dealing with complex chemicals. In these processes PAHs are not removed, but are merely transferred to another phase, up-concentrated and treated as a waste stream.

One of the byproducts during the metal reduction process is energy-rich off-gas and usually this energy is not harnessed. SINTEF Materials and Chemistry along with Ferroalloy industry is developing a novel concept for energy recovery from ferroalloy furnaces. The concept is based on the idea of introducing a combustion chamber in the off-gas section, in which controlled combustion of process gas will be carried out. A

combustion chamber will be designed in which the process gas consisting of PAH obtained from furnace will be oxidized with air. This oxidation process is performed inside a combustion chamber and the design of the combustion chamber has been presented elsewhere (Panjwani 2017). The oxidation rate of PAH depends on the local temperature and reaction kinetics of the PAH. There is a plethora of kinetic data available on the formation of PAH during pyrolysis or combustion, but the kinetic data on mechanisms dealing with oxidation of PAH are very limited. It has become apparent that PAH combustion at high temperature is not the most actively studied field, but rather closely related fields such as PAH and soot formation from smaller hydrocarbons as well as room temperature atmospheric oxidation of PAHs. Such related studies do contain highly relevant data for the study of PAH combustion as well, but care must be taken to find and extract relevant data on the complete combustion of PAHs. The paper by Mati et al. (Mati et al. 2007) stands out in this respect, reporting on a study of 1-methylnaphthalene combustion involving both experiments as well as including a kinetics model with 146 species and 1041 reactions. The kinetic data used in the model consists of a mixture of literature data and estimated data based on chemical considerations and similar reactions wherever literature data were unavailable. The oxidation of methylnaphthalene has been performed experimentally by Mati et al. in a Jet stirred Reactor (JSR) over a wide range of temperatures (800–1421 K) at 1 atm and 10 atm pressure, and residence times 0.5 to 1.5 s. The 1-methylnaphthalene kinetic mechanism consists of 146 species and 1041 elementary reactions. There is also a wealth of useful kinetics models from the CRECK Modelling group (http://creckmodeling.chem.polimi.it/) in Milan who deal with kinetics modelling of combustion and pyrolysis systems involving, e.g., conversion from coal and biomass to PAHs and small molecules as well as from small hydrocarbons to PAHs and soot.

An accurate prediction of PAH combustion inside a combustion chamber requires a coupling between complex chemical kinetics and CFD. Incorporating reaction kinetics of 1-methylnaphthalene within Computational Fluid Dynamics (CFD) requires solving around 150 transport equations which is indeed computationally demanding and the computational cost will increase further when including more complex PAH. Therefore a simplified approach is developed in which oxidation of 1-methylnaphthalene is studied independently at different pressures, temperatures and species concentration. It is assumed that the oxidation of PAH will not affect the overall flow pattern or temperature. The temperature, pressure and species concentration including PAH concentration will be obtained from the CFD simulation of a combustion chamber. The present study is divided into two parts. In part-1, the kinetic study using a perfectly stirred reactor is performed to estimate a minimum residence time and temperature required for oxidation of 1-methylnaphthalene in the presence of process gas consisting of mainly CO and H_2O. This information has been used for the sizing of the combustion chamber[1]. In part-2, the oxidation of 1-methylnaphthalene inside the combustion chamber will be assessed using the Chemical Reactor Network (CRN) approach (Falcitelli et al. 2002; Fichet et al. 2010; Skjøth-Rasmussen et al. 2004). An algorithm to construct CRN was proposed by Falcitelli et al. (Falcitelli et al. 2002) They showed that this methodology could be successfully applied to several industrial cases and in each case, the NOx prediction presents a great accuracy compared to measurements with less than a 5% error.

EXPERIMENTAL AND THEORETICAL SOURCES OF KINETIC DATA

Even though there is a limited amount of literature data on kinetics, one can find data on PAH oxidation in for instance the atmospheric chemistry literature, which deals with reactions of a large number of different PAHs emitted to the atmosphere (Keyte, Harrison, and Lammel 2013; Saggese et al. 2014). The most well studied oxidizing species are OH, O_3, and NOx. One must remember that contrary to combustion, such reactions, typically studied at room temperature, give only partially oxidized PAH derivatives rather than leading to complete destruction. These reaction products are of particular interest not only as intermediates in the degradation of PAHs, but also since they potentially are more toxic than the parent PAHs. The crucial rate-determining steps are in these cases found in the first few reaction steps of PAH oxidation, since the products generally are more reactive than the PAHs themselves.

Reactions with OH will be particularly relevant if there is a significant amount of water vapour is available in the gas. With some caution the room temperature kinetic data could be extrapolated to combustion conditions. A useful support in this case is to complement experimental data with atomic-scale quantum chemistry calculations, as has been performed on the oxidation of naphthalene (Qu, Zhang, and Wang 2006; Zhang, Lin, and Wang 2012). Such calculations can be used to directly calculate activation energies, allowing for safer extrapolation of kinetic data from one temperature to another. One should just be careful to validate the calculated data against reliable benchmark literature data as far as possible. Such comparisons have for instance been made for the chemically related initial steps of benzene oxidation (Taatjes et al. 2010).

ALTERNATIVE PROCESSES FOR PAH OXIDATION AND DESTRUCTION

One alternative way of oxidizing PAHs is to use suitable catalysts. Recent work by Varela-Gandía et al. (Varela-Gandía et al. 2013) focused on achieving complete oxidation of naphthalene by using palladium nanoparticles protected by polymers sitting in porous support materials, such as zeolites and alumina. The results were very promising and 100% conversion was achieved between 165°C and 180°C. Best performance and stability were found using the BETA zeolite as support.

A number of research groups are also working on plasma-assisted conversion of PAHs (Chun, Kim, and Yoshikawa 2011; Odeyemi, Rabinovich, and Fridman 2012; Yu, Li, et al. 2010; Yu, Tu, et al. 2010). The studies by Yu et al.(Yu, Li, et al. 2010; Yu, Tu, et al. 2010) report on the destruction of naphthalene, acenaphthene, fluorene, anthracene and pyrene in a direct current gliding arc plasma reactor at a temperature of 130°C. The PAHs are found to be destroyed to within 93-98% in pure oxygen, with slightly lower values in air. The products are mainly CO, CO_2, H_2O and O_3. In air a rather significant amount of NOx is also formed along with partially oxidized PAH molecules containing keto and NO_2 groups. These PAH derivatives will likely react further much more readily than the parent PAH molecules.

METHOD AND TOOLS:

The residence time and flame temperature are very important for designing the combustion system. These two parameters are estimated using a perfectly stirred reactor (PSR) (Ellen M. 1996). The PSR is an ideal reactor in which uniform mixing is assumed inside the control volume due to diffusion and forced turbulent mixing. This means the rate of reaction is mainly governed through chemical kinetics and not through mixing. In other words the mixing time scale is much shorter than the chemical time scale. The residence time (τ) inside the reactor is defined as $\tau = \frac{V_r}{\dot{m}}$, where V_r is volume of the reactor. Figure 1 illustrates the conceptual representation of the reaction, where the reactant is introduced at the inlet with specified temperature and species concentration. The reactants are ignited inside the reactor at constant pressure. The product will be formed depending on the kinetic of the reactants.

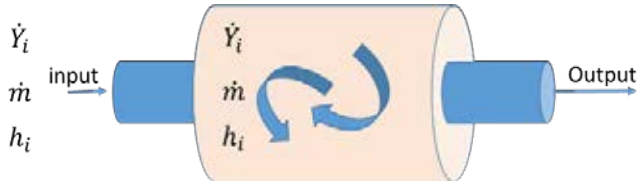

Figure 1 Schematic of PSR

The product leaving the reactor has a certain composition and temperature. If the residence time is too short or the temperature is too low there will be an insignificant amount of reactions occurring and in that situation the outlet properties (temperature and species composition) will be same as those of the inlet. Before using the PSR concept for more realistic problems a verification test case is performed. A suitable test case for verification of the PSR approach would be oxidation of a hydrocarbon. Here, an oxidation study of methane with air at different equivalence ratio (phi) is performed using the PSR code. Figure 2 illustrates the comparison of the present study (symbol) with literature data (solid line) (W.-C. Chang and J.-Y. Chen). The results show that the reactor temperature is well predicted for both lean (phi=0.7) and rich (phi=1.2) fuel conditions for an initial temperature of 295K and atmospheric pressure.

OXIDATION CHARACTERISTIC OF PAH

The oxidation of a PAH is mainly governed by temperature and residence time and will only take place if temperature and residence time are above critical values. These critical values depend on the kinetic data of the PAH itself. In the mechanism (Mati et al. 2007), the initiation reactions for the oxidation of methylnaphthalene includes C-H bond cleavage yielding the methylnaphtyl radical ($C_{10}H_7CH_2$).

$$C_{10}H_7CH_3 = C_{10}H_7CH_2 + H$$

A detailed description involving the different chains of reactions and intermediate products has been given by Mati et al. (Mati et al. 2007). It is worth mentioning that the oxidation of 1-methylnaphthalene also produces many complex intermediate such as Indene, A2R5C2H, A3R5AC, etc. The stoichiometric chemical reaction between 1-methylnaphthalene and air is given below. Oxidation of 1 mole of methylnaphthalene requires 13.5 mole of air.

$$C_{10}H_7CH_3+13.5(O_2+3.76N_2) = 10CO_2+5H_2O+50.76N_2$$

While performing PSR simulations; 0.0153 moles of $C_{10}H_7CH_3$, and 0.207 moles of O_2 and 0.77 moles of N_2 were fed at the inlet of PSR reactor. For a given inlet the temperature and pressure of the reactor were maintained constant but the residence time was increased from 0.2 to 2 s. The resulting output of the PSR was mole fractions of the reactant and product. Figure 3 illustrates 1-methylnaphthalene mole fraction (y-axis log scale) as a function of residence time at temperature from 800-1600^{0}C. The results show that the oxidation of 1-methylnaphthalene will not take place below 800^{0}C and a residence time shorter than 0.2 s. For a given inlet temperature, the increase in residence time accelerates the rate of oxidation of 1-methylnaphthalene. Figure 4 illustrates the CO_2 mole fraction (y-axis log scale) as a function of residence time at different temperature (800-1600 ^{0}C). The formation rate of CO_2 is also very small at temperatures below 800^{0}C since there are no reactions occurring at this temperature.

The results obtained from this study have been utilized for sizing of the combustion chamber (Panjwani 2017). While designing the combustion chamber it was ensured that the temperature inside the combustion chamber is not lower than 800 ^{0}C and that the residence time of the PAH component should be more than 2 s. Current study was useful for finding intermediate during the oxidation of PAH. The detail of the full combustion chamber design in not presented here but a simplified 2D axisymmetric design is presented and discussed here. The simplified design is used for understanding the PAH oxidation. The results from the study will make a platform for designing the full scale 3D combustion chamber design.

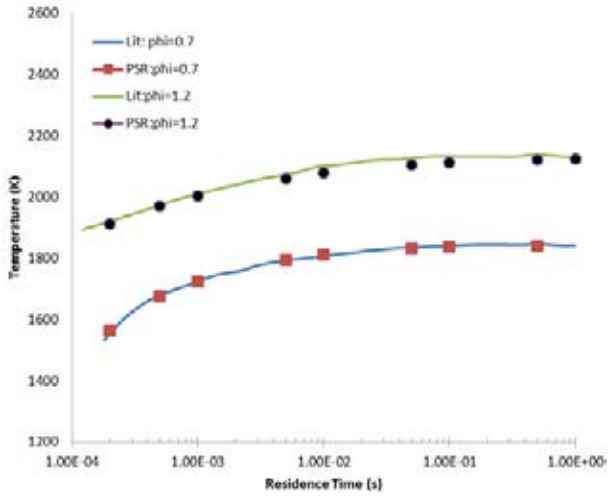

Figure 2 Effect of residence time on the reactor temperature

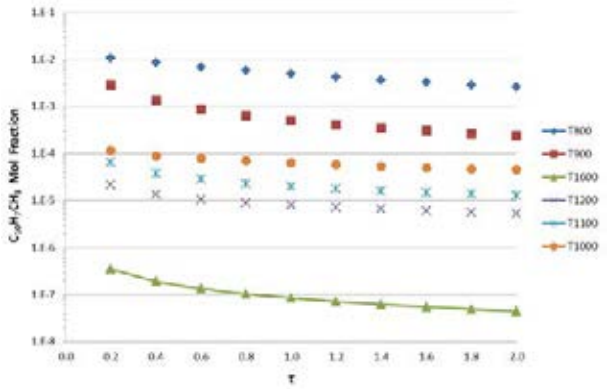

Figure 3 Mole fraction of 1-methylnaphthalene at different temperature as a function of residence time

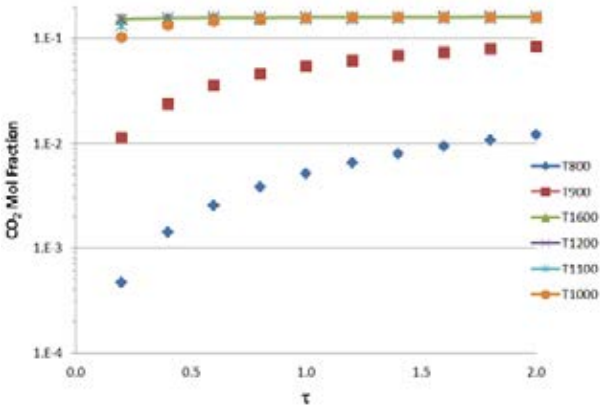

Figure 4 CO_2 mole fraction at different temperature as a function of residence time

GEOMETRY AND MODELLING SETUP

The design and operation of the combustion chamber depend on many parameters, including the total power capacity of the combustion chamber, and the residence time for combusting the complex PAH, NOx. The process gas mainly consists of CO, H_2O, CO_2 and Si components in a Ferro Silicon furnace and Mn components in a Ferro Manganese furnace. The process gases also consist of a certain amount of PAH and the treatment of these PAH is a challenge due to their stable complex rings. Axisymmetric combustion chamber has been be proposed for PAH oxidation.

A CFD-based approach has been used for designing the combustion chamber. CFD has become mature enough to be used for designing any industrial or laboratory scale system involving flow, heat and mass transfer. The commercial CFD software ANSYS FLUENT (ANSYS 2016) has been utilized for this purpose.

An axisymmetric combustion chamber with primary and secondary inlets for air has been proposed (see Figure 5). The geometry and mesh were generated using the ANSYS design modeler. The generated mesh was imported into the FLUENT (Finite Volume Solver). In the model setup, the convective and diffusive terms in the transport equation were discretized using second-order schemes. The turbulence-chemistry was modeled with the eddy dissipation concept model. Turbulence was handled with the k-ε model and for radiation a well-known Discrete Ordinance (DO) model was employed. The process gas mainly consists of 70-75% of CO and 20-25 % of H_2O. The oxidation mechanism of CO with air was modeled using a detailed chemical kinetic mechanism involving 12 species and 28 elementary reactions (Drake and Blint 1988). Pressure-velocity coupling was achieved by the SIMPLE algorithm. The PAH modelling principle described in the earlier sections has only been validated for one set of conditions such as pressure, temperature and species concentration. However, in the actual combustion chamber all these parameters i.e. pressure, temperature, species concentration, residence time and PAH concentration vary with time and space. CFD modelling of complex hydrocarbons having hundreds of species and thousands of reaction mechanisms is a computationally demanding task.

Furthermore, performing CFD simulation for several flow conditions will be a daunting task. In the present study an approach called chemical reactor network (CRN) analysis is utilized in which flow parameters such as concentrations of major species (CO, CO_2, H_2O), temperature and pressure are extracted from the CFD simulation. These variables are subsequently supplied to a stand-alone reactor. In principle each numerical cell of the CFD is treated as a PSR. Here we assumed that the temperature and concentration changes due to oxidation of the PAH has insignificant effects on the global flow parameters i.e. velocity, temperature and pressure. The approach has previously been applied to different furnace geometries, such as pilot-scale and full scale boilers, low-NOx burner flames, incinerators and glass furnaces. A similar approach was introduced by Skjøth-Rasmussen et al. (Skjøth-Rasmussen et al. 2004) who solved larger geometrical problems considering each computational cell of the CFD grid as a perfectly stirred reactor. The results obtained from this approach were encouraging therefore this approach is utilized for current study.

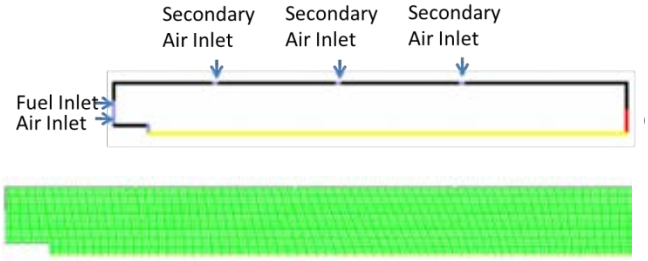

Figure 5 Geometry and Mesh of the combustion chamber

RESULTS AND DISCUSSION

Results obtained from CFD simulations without PAH oxidation is presented. The temperature distribution on the middle plane of the combustion chamber is shown in Figure 6. There are mainly four hot pockets, one close to the primary air inlet and the remaining three hot pockets are close to the secondary air inlets. The maximum temperature is around 1700^0C for a chosen fuel/air ratio. The peak temperature varies for different fuel/air compositions.

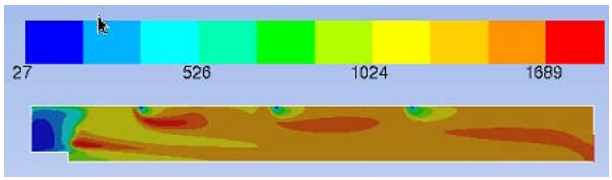

Figure 6 Contours of Static Temperature (^{0} C)

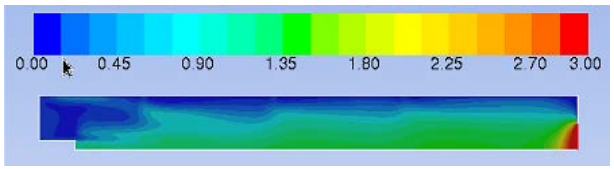

Figure 7 Contours of velocity magnitude (m/s)

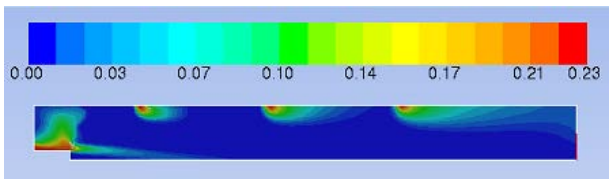

Figure 8 Contours of O2 mass fraction (-)

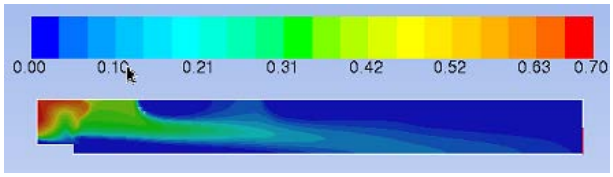

Figure 9 Contours of CO mass fraction (-)

Ignition of the process gas starts when it comes into contact of fresh air. The magnitude of velocity is shown in Figure 7. The average velocity is around 1.5 m/s and the maximum exit velocity is around 3 m/s. A distribution of O_2 mass fraction is shown in Figure 8. The maximum mass fraction is close to the inlet. It can be observed that air is not able to penetrate due to strong axial momentum force. As soon as air is injected from the secondary inlets it is subjected to an axial force and it follows along the direction of the combustion chamber. The incoming CO mixes with the air and starts combusting close to the secondary air inlets. A contour plot of CO mass fraction is shown in Figure 9. It can be seen that the CO mass fraction is much higher ahead of the secondary air inlets. The CO will start combusting when it mixes with air coming from the secondary air inlets.

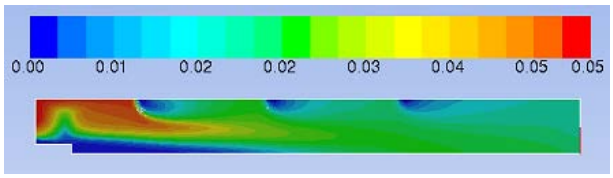

Figure 10 Contours of PAH mass fraction (Without any oxidation)

A contour of PAH distribution without any oxidation is shown in Figure 10. In the CFD study PAH is behaving as a non-reacting species because an oxidation process of PAH is not considered. This PAH concentration along with other species such O_2, N_2, CH_4, CO_2, CO will be input to the PSR reactor model. As mentioned earlier, each numerical cell of the CFD is treated as a PSR. The major output from the PSR reactor model will be change in PAH, O_2, N_2, CH_4, CO_2, CO concentration and intermediate species concentration. It is assumed that the flow is frozen and in steady state and effect of change in temperature and species concentration due to PAH oxidation is insignificant on the global flow field.

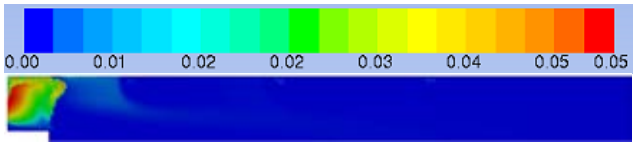

Figure 11 Contours of PAH mass fraction (after PSR simulations)

Results from CRN analyses is shown in Figure 11, which is illustrating the contours of PAH mass fraction after PSR simulation. Higher mass fraction can be observed at entrance of the combustion chamber due to unavailability of the oxidizer, lower temperature and lower residence time. As we move further downstream, the PAH concentration keeps on diminishing. It should be mentioned that during the PSR calculation a residence time of 2 s was assumed everywhere. In reality, however, this residence time will be a function of space. This varying residence time might have some impact on the PAH concentration but is not considered in the present study.

CONCLUSIONS

Estimating the chemical kinetics data of PAH is a challenging task. An extensive literature survey was performed for finding the chemical kinetic data of PAH and based on this study we were only able to find kinetic data for 1-methylnaphthalene. A PSR simulation of 1-methylnaphthalene for a given set of chemical mechanisms clearly indicates that the combustion of 1-methylnaphthalene depends on the residence time and

initial temperature. The minimum temperature at which combustion of 1-methylnaphthalene starts is around 800^0C. This study shows that the effect of residence time is weaker than the effect of temperature on the combustion of 1-methylnaphthalene. A residence time of 2s is essential for the oxidation of methylnaphthalene. A CRN analysis approach is utilized for understanding the oxidation of PAH inside the combustion chamber. The oxidation of PAH occurs at much longer time scales than the oxidation of process gas, which occurs on time scales on the order of micro- to milli-seconds. The study clearly showed that almost all the PAH is oxidized as far as 1-methylnaphthalene is concerned. However, we do not have any kinetic data on the complex PAHs and with the present results we cannot make definite conclusions about the oxidation behavior of these more complex species.

ACKNOWLEDGMENT

The research work carried out in this article is funded by SCORE (Staged Combustion for Energy Recovery in Ferroalloy industry) project funded by Norwegian research council and The Norwegian Ferroalloy Producers Research Association (Ferrolegeringsindustriens Forskningsforening (FFF)). Funding from the SCORE project is greatly acknowledged

REFERENCES

ANSYS, INC. 2016. *ANSYS FLUENT Theory Guide*.

Chun, Young Nam, Seong Cheon Kim, and Kunio Yoshikawa. 2011. 'Destruction of anthracene using a gliding arc plasma reformer', *Korean Journal of Chemical Engineering*, 28: 1713.

Drake, Michael C., and Richard J. Blint. 1988. 'Structure of Laminar Opposed-flow Diffusion Flames With CO/H2/N2 Fuel', *Combustion Science and Technology*, 61: 187-224.

Ellen M., Harry K. M., Joseph F. G., and Robert J. K. 1996. "A FORTRAN Program for Modeling Well Stirred Plasma and Thermal Reactors with Gas and Surface Reactions " In.: Sandia.

Falcitelli, M., S. Pasini, N. Rossi, and L. Tognotti. 2002. 'CFD+reactor network analysis: an integrated methodology for the modeling and optimisation of industrial systems for energy saving and pollution reduction', *Applied Thermal Engineering*, 22: 971-79.

Fichet, Vincent, Mohamed Kanniche, Pierre Plion, and Olivier Gicquel. 2010. 'A reactor network model for predicting NOx emissions in gas turbines', *Fuel*, 89: 2202-10.

Keyte, Ian J., Roy M. Harrison, and Gerhard Lammel. 2013. 'Chemical reactivity and long-range transport potential of polycyclic aromatic hydrocarbons - a review', *Chemical Society Reviews*, 42: 9333-91.

Mati, Karim, Alain Ristori, GaËLle Pengloan, and Philippe Dagaut. 2007. 'Oxidation of 1-Methylnaphthalene at 1–13 atm: Experimental Study in a JSR and Detailed Chemical Kinetic Modeling', *Combustion Science and Technology*, 179: 1261-85.

Odeyemi, F., A. Rabinovich, and A. Fridman. 2012. 'Gliding Arc Plasma-Stimulated Conversion of Pyrogas into Synthesis Gas', *IEEE Transactions on Plasma Science*, 40: 1124-30.

Panjwani, B., Wittgens, B., Olsen, J.E. 2017. "COMBUSTION CHAMBER SCALING FOR ENERGY RECOVERY FROM FURNACE PROCESS GAS: WASTE TO VALUE " In.

Qu, Xiaohui, Qingzhu Zhang, and Wenxing Wang. 2006. 'Mechanism for OH-initiated photooxidation of naphthalene in the presence of O2 and NOx: A DFT study', *Chemical Physics Letters*, 429: 77-85.

Saggese, Chiara, Nazly E. Sánchez, Alessio Frassoldati, Alberto Cuoci, Tiziano Faravelli, María U. Alzueta, and Eliseo Ranzi. 2014. 'Kinetic Modeling Study of Polycyclic Aromatic Hydrocarbons and Soot Formation in Acetylene Pyrolysis', *Energy & Fuels*, 28: 1489-501.

Skjøth-Rasmussen, M. S., O. Holm-Christensen, M. Østberg, T. S. Christensen, T. Johannessen, A. D. Jensen, P. Glarborg, and H. Livbjerg. 2004. 'Post-processing of detailed chemical kinetic mechanisms onto CFD simulations', *Computers & Chemical Engineering*, 28: 2351-61.

Taatjes, Craig A., David L. Osborn, Talitha M. Selby, Giovanni Meloni, Adam J. Trevitt, Evgeny Epifanovsky, Anna I. Krylov, Baptiste Sirjean, Enoch Dames, and Hai Wang. 2010. 'Products of the Benzene + O(3P) Reaction', *The Journal of Physical Chemistry A*, 114: 3355-70.

Varela-Gandía, Francisco J., Ángel Berenguer-Murcia, Dolores Lozano-Castelló, Diego Cazorla-Amorós, David R. Sellick, and Stuart H. Taylor. 2013. 'Total oxidation of naphthalene using palladium nanoparticles supported on BETA, ZSM-5, SAPO-5 and alumina powders', *Applied Catalysis B: Environmental*, 129: 98-105.

W.-C. Chang and J.-Y. Chen. 'http://firebrand.me.berkeley.edu/griredu.html', Accessed 28/04/2017.

Yu, Liang, Xiaodong Li, Xin Tu, Yu Wang, Shengyong Lu, and Jianhua Yan. 2010. 'Decomposition of Naphthalene by dc Gliding Arc Gas Discharge', *The Journal of Physical Chemistry A*, 114: 360-68.

Yu, Liang, Xin Tu, Xiaodong Li, Yu Wang, Yong Chi, and Jianhua Yan. 2010. 'Destruction of acenaphthene, fluorene, anthracene and pyrene by a dc gliding arc plasma reactor', *Journal of Hazardous Materials*, 180: 449-55.

Zhang, Zhijie, Ling Lin, and Liming Wang. 2012. 'Atmospheric oxidation mechanism of naphthalene initiated by OH radical. A theoretical study', *Physical Chemistry Chemical Physics*, 14: 2645-50.